

Spin-resolved angle-dependent photoemission study of ordered Fe<sub>3</sub>Pt(001) Invar

C. Carbone, E. Kisker, K.-H. Walker\*

*Institut für Festkörperforschung der Kernforschungsanlage Jülich, D-5170 Jülich, West Germany*

E. F. Wassermann

*Laboratorium für Tieftemperaturphysik, Universität Duisburg, D-4100 Duisburg, West Germany*

(Received 6 October 1986)

The electronic structure of ordered fcc Fe<sub>3</sub>Pt(001) Invar has been studied by spin-resolved, angle-dependent photoemission with synchrotron radiation. The exchange splitting along  $\Delta$  is determined to be  $2.1 \pm 0.2$  eV. The peak positions in the spin-resolved energy distribution curves agree closely with recent band-structure calculations. A close relation to the calculated electronic structure of fcc Fe in the high-spin state is observed.

The temperature invariance of the thermal expansion coefficient over a wide range around room temperature in alloys such as Fe<sub>65</sub>Ni<sub>35</sub> and Fe<sub>3</sub>Pt has been known as the Invar effect for a long time. Conflicting models for understanding the effect have been discussed in the past. On the one hand, there are the local-moment models based on the  $2\gamma$ -state hypothesis of Weiss,<sup>1</sup> which assume that the loss of magnetization is caused by a transition of the iron atoms from a ferromagnetic ground state ( $\gamma_2$ ) to an antiferromagnetic excited state ( $\gamma_1$ ) when  $T_C$  is approached. On the other hand, there are itinerant-electron models, which postulate a reduction of the magnetic moment within the Stoner model and assume that the Invar alloys are weak itinerant ferromagnets.<sup>2</sup> Though a volume decrease accompanies the reduction of the magnetization in both models, their application to explain the Invar anomalies in ordered Fe<sub>3</sub>Pt remain doubtful, since neither magnetic heterogeneity nor weak itinerancy seems to occur in this system.<sup>3</sup> Consequently, it was suggested that there are two types of Invar, the large group of magnetically weak systems like FeNi and the strong ferromagnets Fe<sub>3</sub>Pt and Fe<sub>3</sub>Pd.<sup>4</sup> Detailed spin-dependent band-structure calculations and their experimental tests are therefore required. For ordered Fe<sub>3</sub>Pt, ground-state ( $T=0$ ) electronic-structure calculations have been performed recently by Inoue and Shimizu<sup>5</sup> [giving density of states (DOS) only] and by Hasegawa.<sup>6</sup> The spin-orbit interaction has not been taken into account.

A first test of the electronic structure of disordered FeNi alloys by spin-resolved *threshold* photoemission was performed by Landolt, Niedermann, and Mauri,<sup>7</sup> demonstrating a strong dependence of the spin character of the DOS near  $E_F$  on the Fe concentration. In this Rapid Communication we present the first experimental study of the electronic structure of ordered fcc Fe<sub>3</sub>Pt by spin- and angle-resolved photoemission with synchrotron radiation. The data will also show that there is a close relationship between the electronic structures of ordered Fe<sub>3</sub>Pt (lattice constant  $a=3.75$  Å) and that of pure fcc Fe of comparable lattice constant ( $a=3.70$  Å), i.e., in the so-called "high-spin state."<sup>8</sup> This is of special relevance to the understanding of the Invar effect in ordered Fe<sub>3</sub>Pt.

The experiment has been conducted at the Berliner

Elektronenspeicherring-Gesellschaft für Synchrotron-Strahlung (BESSY) storage ring in West Berlin using the apparatus as described elsewhere,<sup>9</sup> here improved to provide the possibility of rotating the sample around its [100] (rotation angle  $\Phi$ ) and [010] (rotation angle  $\Theta$ ) directions. The surface normal is in the [001] direction.  $\Theta, \Phi=0$  refers to normal emission. The [100] axis is aligned parallel and the [010] axis perpendicular to the fixed light electric vector. With the fixed electron spectrometer, angle-dependent photoemission is possible by rotating the sample. Rotating around  $\Phi$  ( $\Theta=0$ ), the light is kept *s* polarized. Energy resolution was about 0.4 eV, angular resolution about  $\pm 3^\circ$ . The corresponding  $k$  resolution at a photon energy of 60-eV is about  $\frac{1}{4}$  of the length of the  $\Gamma$ - $X$  direction. The achievable  $k$  resolution in the simple cubic lattice is worse than in the fcc one because of the small Brillouin zone of the simple cubic lattice.

A single crystal with composition Fe<sub>72</sub>Pt<sub>28</sub> in the form of a 0.8-mm-thick ellipsoidal disk (axes 12 and 10 mm, respectively), cut parallel to the (001) plane, was used as the sample. To install the order, the sample was cooled from 870 °C to 500 °C at a rate of 1 degree/h. The Curie temperature ( $T_C$ ) in the ordered phase as determined from magnetization measurements is 470 K. A spark-eroded 4-mm center hole provided a ring shape to accomplish magnetic saturation by sending a current pulse through a coil wound around part of the ring.

The sample could be heated by electron bombardment and cooled to about  $-25^\circ\text{C}$ . It was cleaned *in situ* by repeated Ne<sup>+</sup> ion etching and annealing cycles. Surface composition was checked by Auger electron spectroscopy. After sputtering, a Pt-rich surface was obtained. Flashing to about 770 °C resulted in a surface composition (determined from the Auger electron spectra) of Fe<sub>*x*</sub>Pt<sub>1-*x*</sub>,  $x=0.66 \pm 0.05$ , which is close to the chemical composition of the bulk material and is still in the Invar regime. From the temperature dependence of the secondary-electron spin polarization (measured *in situ*),  $T_C=450$  K is obtained, corresponding to a degree of order of between 60% and 70%.<sup>10</sup>

Figure 1(a) shows the spin-integrated energy distribution curve (EDC)  $I(E) = I^{\uparrow}(E) + I^{\downarrow}(E)$  at 60-eV photon

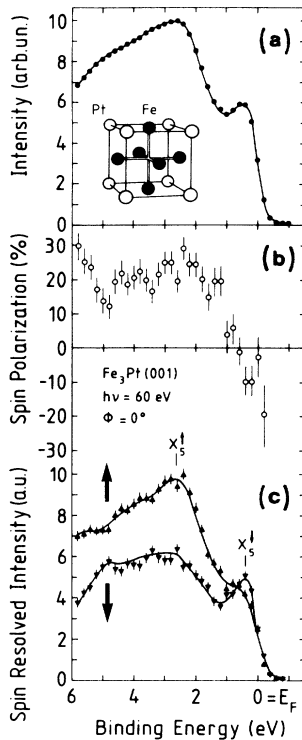


FIG. 1. (a) Spin-integrated energy distribution curve (EDC) for normal emission and normal-incident light from ordered  $\text{Fe}_3\text{Pt}(001)$  at 60-eV photon energy. (b) Spin polarization curve corresponding to (a). (c) Spin-resolved EDC's.

energy for normal-emission and normal-incidence light, Fig. 1(b) the corresponding spin-polarization curve  $P(E) = (I^\uparrow - I^\downarrow) / (I^\uparrow + I^\downarrow)$ , and Fig. 1(c) the spin-resolved EDC's  $I^\uparrow(E), I^\downarrow(E)$ .  $\uparrow$  refers to majority-spin electrons.

The spin polarization is negative at  $E_F$  and becomes positive at about 0.8-eV binding energy ( $E_B$ ). The maximum positive value of about 25% is obtained around  $E_B = 2.5$  eV. It has been found that the polarization amplitude depends strongly on the sample surface conditions. Flashing to about 770 °C is necessary to obtain the comparatively high spin polarization as in Fig. 1(b). In the spin-integrated EDC [Fig. 1(a)] the height of the peak near  $E_F$ , relative to that at 2.6 eV rather than the peak positions, depends on the annealing temperature.

Main features in the spin-resolved EDC's [Fig. 1(c)] are a dominant majority-spin ( $\uparrow$ ) peak near  $E_B = 2.6 \pm 0.2$  eV and a peak in the minority-spin ( $\downarrow$ ) EDC at  $E_B = 0.5 \pm 0.2$  eV. There are, reproducibly, other weaker structures as, e.g., the shoulder slightly below  $E_F$  in the  $\uparrow$ -spin EDC and a broad feature around  $E_B = 3$  eV in the  $\downarrow$ -spin EDC.

We display in Fig. 2(a) spin-integrated EDC's as obtained at two different emission angles,  $\Phi = 0^\circ$  and  $\Phi = 14^\circ$ , and in Fig. 2(b) the corresponding spin-resolved curves. With increasing azimuthal angle, the dominating  $\uparrow$ -spin peak shifts from  $E_B \approx 2.6$  to  $E_B \approx 3.1$  eV. The  $\downarrow$ -spin peak near  $E_F$  also shifts to lower energy by the same

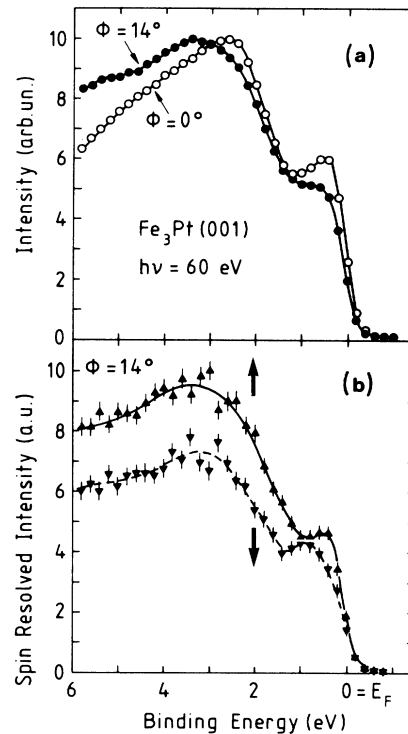


FIG. 2. (a) Spin-integrated EDC's for  $s$ -polarized light from ordered  $\text{Fe}_3\text{Pt}(001)$  at 60-eV photon energy at azimuthal angles  $\Phi = 0^\circ$  and  $\Phi = 14^\circ$ . (b) Spin-resolved EDC's at  $\Phi = 14^\circ$ .

amount. This occurs also when rotating the sample around the  $\Theta$  axis. The similar dependence of the two peaks on emission angle suggests that they have similar wave-function symmetries and that they represent, accordingly, a pair of exchange-split states.

In Fig. 3, we display spin-resolved EDC's taken at 90-eV photon energy. The main difference to the 60-eV data is an increase in  $\uparrow$ -spin intensity near  $E_F$ , resulting also in a larger amplitude of the spin-integrated peak below  $E_F$  [cf. Figs. 1(a) and 3(a)]. The smallest binding energy (2.1 eV) of the dominating peak in the  $\uparrow$ -spin EDC is observed at  $h\nu = 28$  eV.

For comparison with our photoemission data, the relevant part (along  $\Gamma$ - $X$ ) of the spin-polarized band structure for ordered  $\text{Fe}_3\text{Pt}$  as calculated by Hasegawa<sup>6</sup> is shown in Figs. 4(a) and 4(b). Free-electron-like final states for the simple cubic  $\text{Fe}_3\text{Pt}$  lattice are shown in Fig. 4(c). Accordingly, the initial states are near the middle of the Brillouin zone at  $h\nu = 28$  eV, close to  $X$  at 60 eV, and near  $\Gamma$  at 90 eV. Because of (nonrelativistic) dipole selection rules, bands of  $\Delta_5$  symmetry are allowed as initial states for normal-emission and  $s$ -polarized light.<sup>11</sup> Bands of this symmetry are, therefore, expected to dominate in the spectra. However, bands with a high density of states and  $k$  vectors close to the  $\Gamma$ - $X$  direction also contribute to the spectra [cf. similar studies on bcc  $\text{Fe}(100)$  (Ref. 9)].

The discussion has shown that at  $h\nu = 60$  eV, the  $\uparrow$ -spin peak at  $E_B = 2.6$  eV and the  $\downarrow$ -spin peak at  $E_B = 0.5$  eV [Fig. 1(c)] represent exchange-split states with splitting of

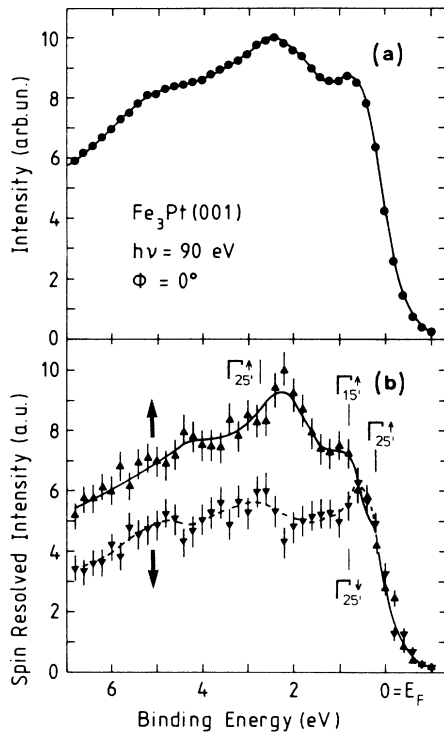


FIG. 3. (a) Spin-integrated EDC for normal emission and normal-incident light from ordered  $\text{Fe}_3\text{Pt}(001)$  at 90-eV photon energy. (b) Spin-resolved EDC.

$2.1 \pm 0.2$  eV. The minimum in  $\downarrow$ -spin intensity around  $E_B = 1.6$  eV corresponds to a gap in allowed initial states between about 1 and 2 eV [see Fig. 4(b)]. The  $\uparrow$ -spin intensity between  $E_F$  and  $E_B \approx 1$  eV is attributed to the very flat bands of  $\Delta_2^{\uparrow}$  and  $\Delta_1^{\uparrow}$  symmetries ( $E_B = 0.1$  and 0.8 eV, respectively<sup>6</sup>). Intensity in this energy range is larger at  $h\nu = 90$  eV (initial states near  $\Gamma$ ) than at  $h\nu = 60$  eV (initial states near  $X$ ) because of degeneracy with dipole-allowed bands of  $\Delta_5^{\uparrow}$  symmetry at  $\Gamma$  [Fig. 4(a)].

At  $\Phi = 14^\circ$  emission angle and 60-eV photon energy (Fig. 2), the internal photoelectron wave vector  $\mathbf{k}$  includes an additional component

$$[(2m/\hbar^2 E_{\text{kin}})]^{1/2} \sin\Phi = 0.92 \text{ \AA}^{-1}$$

parallel to the surface in the [010] direction which amounts to about a reciprocal-lattice vector ( $0.84 \text{ \AA}^{-1}$ ). Allowing for the uncertainty in the normal component of  $\mathbf{k}$  due to the presence of the surface, it follows that  $\mathbf{k}$  is along  $X$ - $M$ . Within the direct-transition model,  $\mathbf{k}$  is then determined to be near  $M$ , assuming free-electron final states. The observed binding-energy shifts agree indeed with calculated band energies near  $M$  (not shown in Fig. 4).<sup>6</sup>

In Figs. 4(a) and 4(b), we compare the peak positions obtained from the spin-resolved EDC's with calculated band energies.<sup>6</sup> The agreement is reasonably good considering that the calculation neglects spin-orbit interaction which could be important due to the high  $Z$  value of Pt. The fact that the exchange-split peaks are observed within

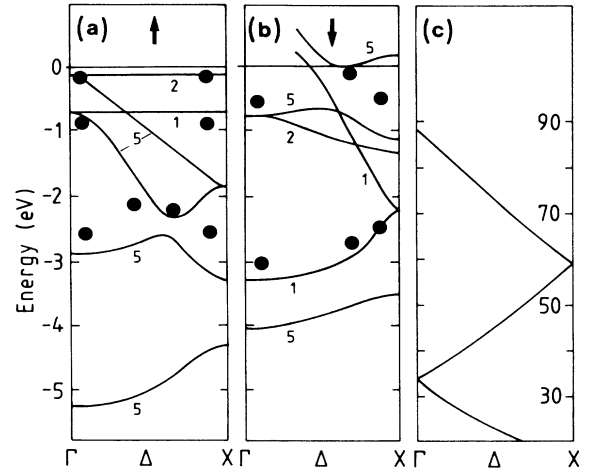


FIG. 4. Comparison of peak positions ( $\bullet$ ) in spin-resolved EDC's at selected photon energies between 28 and 90 eV with calculated band energies of ordered  $\text{Fe}_3\text{Pt}$  (after Ref. 6). (a) Majority-spin bands. Only dipole-allowed bands and others with high partial density of states are shown for clarity. (b) Minority-spin bands. (c) Free-electron bands (spin averaged) in the simple cubic lattice.

the hybridization gaps of the  $\Delta_5^{\uparrow, \downarrow}$  bands ( $E_B \approx 0.5$  and 2.6 eV, respectively) might suggest a relation to surface states, but changes in peak positions have not been observed in runs with different surface treatments, or after residual gas contamination.

We have compared our data obtained for a sample with 60–70% degree of order with the band structure for the fully ordered system. The main effect of disorder is probably a smearing of the wave vector and a broadening of the structures since  $k$  is less well defined in the presence of disorder.

Because of the similarity in the crystal structures of  $\text{Fe}_3\text{Pt}$  and pure fcc Fe [cf. inset in Fig. 1(a)], it is interesting to compare the data with the calculated electronic structure of fcc Fe.<sup>8</sup> The reciprocal lattice of ordered  $\text{Fe}_3\text{Pt}$  is simple cubic with  $\Gamma$ - $X$  distance only half of that of the corresponding fcc lattice. Accordingly, bands of fcc Fe in the right part of the  $\Gamma$ - $X$  direction are folded back toward  $\Gamma$  in the  $\text{Fe}_3\text{Pt}$ , and bands along  $X$ - $W$  add to those along  $\Gamma$ - $X$ . The folded band structure of fcc Fe in the high-spin state ( $a = 3.7 \text{ \AA}$ )<sup>8</sup> and the  $\text{Fe}_3\text{Pt}$  band-structure ( $a = 3.75 \text{ \AA}$ )<sup>6</sup> are, indeed, very similar, having the same splittings of the  $\Delta_5^{\uparrow, \downarrow}$  bands. Our data present the experimental approach which so far is the closest to the electronic structure of the metastable high-spin phase of fcc Fe which is stabilized here by the Pt.<sup>12</sup> The predicted extremely flat  $\uparrow$ -spin band just below  $E_F$  in high-spin fcc Fe along  $X$ - $W$ , observed here in the  $\text{Fe}_3\text{Pt}$  along  $\Gamma$ - $X$ , is considered to be of major importance in the predicted high- to low-spin-state phase transition in fcc Fe.<sup>8</sup>

In conclusion, we present the first spin- and angle-dependent photoemission study of an ordered alloy. We have shown that the Invar alloy  $\text{Fe}_3\text{Pt}$  can be prepared in ultrahigh vacuum to yield a surface with Curie temperature close to that of bulk Invar. The exchange splitting is

resolved near  $\Gamma$  and  $X$ . Binding energies of spin-split electronic states can be interpreted closely in terms of a recent band structure calculation by Hasegawa.<sup>6</sup> The experimental data on the electronic structure of  $\text{Fe}_3\text{Pt}$  also show a close relationship to the predicted electronic structure of fcc Fe in the high-spin state,<sup>8</sup> corroborating the idea of Weiss<sup>1</sup> that the Invar effect is actually a property of fcc Fe.

We wish to thank Professor M. Campagna for his continued interest and support, the Berliner Elektronenspeicherring-Gesellschaft für Synchrotron-Strahlung (BESSY) staff for their help, Dr. H. Bach for preparing the single crystal, and Professor H. Neddermeyer and Dr. T. Paul for hints regarding surface preparation. This work was partially supported by Sonderforschungsbereich 166.

\*Present address: W. C. Heraeus GmbH, D-6450 Hanau, Federal Republic of Germany.

<sup>1</sup>R. J. Weiss, Proc. Phys. Soc. (London) **82**, 281 (1963).

<sup>2</sup>E. P. Wohlfarth, J. Magn. Magn. Mater. **MAG-10**, 120 (1979).

<sup>3</sup>K. Sumiyama, M. Shiga, and Y. Nakamura, J. Magn. Magn. Mater. **MAG-31-34**, 111 (1983).

<sup>4</sup>E. P. Wohlfarth, Y. Nakamura, and M. Shimizu, J. Magn. Magn. Mater. **MAG-10**, 307 (1979).

<sup>5</sup>J. Inoue and M. Shimizu, J. Phys. F **13**, 2677 (1983).

<sup>6</sup>A. Hasegawa, J. Phys. Soc. Jpn. **54**, 1477 (1985).

<sup>7</sup>M. Landolt, Ph. Niedermann, and D. Mauri, Phys. Rev. Lett. **48**, 1632 (1982).

<sup>8</sup>D. Bagayoko and J. Callaway, Phys. Rev. B **28**, 5419 (1983); D. Bagayoko, Ph.D. thesis, Louisiana State University, 1983

(unpublished).

<sup>9</sup>E. Kisker, K. Schröder, W. Gudat, and M. Campagna, Phys. Rev. B **31**, 329 (1985).

<sup>10</sup>Y. Shen, I. Nakai, H. Maruyama, and O. Yamara, J. Phys. Soc. Jpn. **54**, 3915 (1985).

<sup>11</sup>J. Hermanson, Solid State Commun. **22**, 9 (1977).

<sup>12</sup>The electronic structure of fcc Fe films grown epitaxially on Cu(100) has been studied recently by angle-resolved photoemission by A. Amiri Hezaveh, G. Jennings, D. Pescia, R. F. Willis, K. Prince, M. Surman, and A. M. Bradshaw, Solid State Commun. **57**, 329 (1986); M. F. Onellion, C. L. Fu, M. A. Thompson, J. L. Erskine, and A. J. Freeman, Phys. Rev. B **33**, 7322 (1986). Presumably, the low-spin-state phase was obtained at the Cu lattice constant ( $a = 3.61 \text{ \AA}$ ).